



# Effect of reduced graphene oxide amount on the tribological properties of UHMWPE biocomposites under water-lubricated conditions

Alime Çolak<sup>1</sup> · Meryem Göktaş<sup>1,2</sup> · Ferda Mindivan<sup>1,3</sup>

Received: 23 October 2019 / Accepted: 4 February 2020 / Published online: 10 February 2020  
© Springer Nature Switzerland AG 2020

## Abstract

Ultra-high molecular weight polyethylene (UHMWPE) has been broadly utilized in hip and knee artificial implant due to its low friction coefficient, high wear resistance and good biocompatibility. However, some disadvantage properties such as low young's modulus and low load bearing, anti-fatigue capacity limit application areas and wear debris of UHMWPE components cause implant failure. For this reason, reduced graphene oxide (RGO) filler was produced by green synthesis with vitamin C and the influences of RGO filler content on the tribological performance under distilled water lubrication condition were investigated and had been correlated with microstructure. RGO filled UHMWPE biocomposites were fabricated by firstly liquid phase ultrasonic mixing and then hot press molding. The characterization and experiment results revealed that the wear behavior of UHMWPE/RGO biocomposites were not only affected by the lubricant and binder properties of RGO, but also restricted by the content of RGO filler. The RGO filled UHMWPE biocomposites exhibited a lower wear rate and friction coefficient in comparison to the unfilled UHMWPE. The biocomposite with 0.7 wt% of RGO showed good interfacial bonding strength and excellent wear resistance. Furthermore, fatigue wear tracks reduced significantly on the same biocomposite surface. High crystallite size and microhardness value of UHMWPE/RGO-0.7 biocomposite was caused destroy the tribofilm formed on the  $Al_2O_3$  counterface.

**Keywords** Adhesive wear · Crystallite size fatigue wear · Friction coefficient · Microhardness · Wear resistance

## 1 Introduction

Recently, polymer matrix composites were found ever-rising tribological applications such as gears, bearings, seals and artificial joints instead of metals due to their advantages such as low density, easy manufacturability, superior shock, high vibration and self-lubrication [1, 2]. UHMWPE has been widely used for artificial joints due to its clinical performances in the last two decades [3, 4]. On the other hand, UHMWPE has low Young's modulus, low load bearing and anti-fatigue capacity [5]. Therefore, efforts have been put on to improve tribological performances of

UHMWPE. Incorporation of fillers to overcome shortcomings of the UHMWPE matrix is a promising solution [6]. For this purpose, composite materials were produced using inorganic fillers such as kaolin, zirconium, nano zinc oxide and also, various organic fillers, including carbon fiber, carbon black and carbon nanotubes have been investigated in UHMWPE matrix due to their good surface adherence and better solid lubrication properties. However, these fillers limited their application at UHMWPE composites because of high cost and inadequate performance of composites in artificial joints [5]. Graphene has attracted as an ideal filler recently because of its special properties

✉ Ferda Mindivan, ferda.mindivan@bilecik.edu.tr | <sup>1</sup>Biotechnology Application and Research Centre, Bilecik Seyh Edebali University, 11230 Bilecik, Turkey. <sup>2</sup>Department of Metallurgy, Vocational College, Bilecik Seyh Edebali University, 11230 Bilecik, Turkey. <sup>3</sup>Department of BioEngineering, Faculty of Engineering, Bilecik Seyh Edebali University, 11230 Bilecik, Turkey.



graphene has potential applications in many fields such as composite materials [7]. Commonly, graphene derivatives such as graphene oxide (GO), reduced graphene oxide (RGO), graphene nanoplates (GNP) and multi-layer graphene (MLG) are widely used as fillers for polymer composite materials [8]. GO is prepared from oxidation of graphite powder by Hummers method and RGO is synthesized from the reduction process of GO. Usually, GO and RGO are more preferred than other graphene derivatives due to their hydrophilicity, ease of formation of stable colloidal suspensions and easy-inexpensive synthesis [9]. At the same time, they have antibacterial properties and they were often used for biomedical applications recently [10]. There are studies to investigate tribological properties of UHMWPE composites by using GO [5, 11–13] and GNP [14, 15] but to the best of our knowledge, there are no report on the green synthesis of RGO for UHMWPE and their effects on the tribological properties of UHMWPE biocomposites, in the literature. Bhattacharyya et al. reported that UHMWPE nanocomposite films was produced with RGO using two different process routes. But they used phenylhydrazine as reduction agent. Phenylhydrazine that hydrazine derivative is highly toxic and instability. Therefore, it is not suitable for biomaterial application areas whether excess hydrazine is not removed [16]. In this paper, RGO filler was produced by green synthesis with vitamin C. RGO filled UHMWPE biocomposites were prepared, and the effect of the RGO content of the biocomposites on the structural and tribological properties under distilled water lubrication conditions were investigated. As a consequence, tribological and mechanical properties of UHMWPE can be altered by changing loading content of RGO. Moreover, the synthesized RGO may be a good candidate for UHMWPE based biomaterials.

## 2 Experimental methods

Firstly, GO was prepared by oxidizing the graphite powder according to a modified Hummers' method [8, 17]. The detailed information about the reduction process of GO was described in previous literature [18]. UHMWPE/RGO biocomposites of different weight percentage of RGO to UHMWPE were prepared as follows: In brief, as-prepared powder RGO were sonicated for 30 min in ethyl alcohol using a homogenizer to form a well dispersed suspension. After that, UHMWPE powders were added into the suspension and the mixture was stirred for 30 min and then sonicated for 1 h. Then the ethyl alcohol was removed at 60–70 °C in an oil bath and the biocomposite powders were dried in an oven at 60 °C. Finally, the unfilled UHMWPE and biocomposite powders were molded by hot-pressing at 180 °C under a 10 MPa pressure and holding at

this pressure for 30 min. In order to investigate the effects of RGO on the tribological properties of the biocomposites with the RGO content of unfilled, 0.7 and 3.0 wt% RGO were prepared. The codes of unfilled UHMWPE and these two biocomposites were UHMWPE, UHMWPE/RGO-0.7 and UHMWPE/RGO-3.0. The crystallinity of the biocomposites were represented by X-ray diffraction (XRD) patterns acquired by a PAN analytical, Empyrean diffractometer using Cu K $\alpha$  radiation in the angle range  $2\theta = 5\text{--}30^\circ$ . The molecular structure of the biocomposites were characterized by Fourier transfer infrared spectroscopy (FTIR) spectra which is recorded by a Spectrum 100, Perkin Elmer between 400 and 4000  $\text{cm}^{-1}$ . Shimadzu microhardness tester was used to measure the hardness of the biocomposites prepared. The hardness values were calculated based on the Vickers method with a load of 25 g. At least ten successive measurements were performed for each condition. The scanning electron microscope (SEM) (Zeiss, Supra 40VP) and energy-dispersive X-ray spectrometry (EDS) were used to observe morphology and worn surfaces of the biocomposites. A ball-on-disc reciprocating tribometer was used for all friction and wear tests. Wear tests were performed in a reciprocating mode with a 1.7  $\text{cm s}^{-1}$  sliding rate under 5 N applied load for 45 min. The counter body was an  $\text{Al}_2\text{O}_3$  ball with 10 mm diameter. Following the wear tests, the  $\text{Al}_2\text{O}_3$  counterface surfaces were examined under an optical microscope (OM) in order to investigate the wear mechanisms.

## 3 Results and discussion

Figure 1 showed the XRD diffractograms of unfilled UHMWPE and UHMWPE/RGO biocomposites. The two peaks at  $2\theta = 21.56$  and  $2\theta = 23.92$ , that appear in all diffractograms, correspond to the (110) and (200) planes of the orthorhombic crystal [19]. Inclusion of 0.7 wt% and

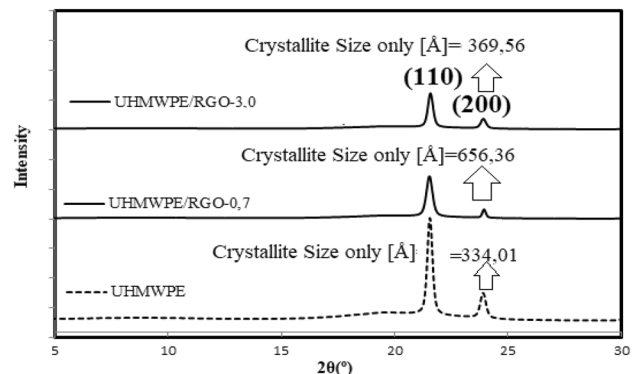
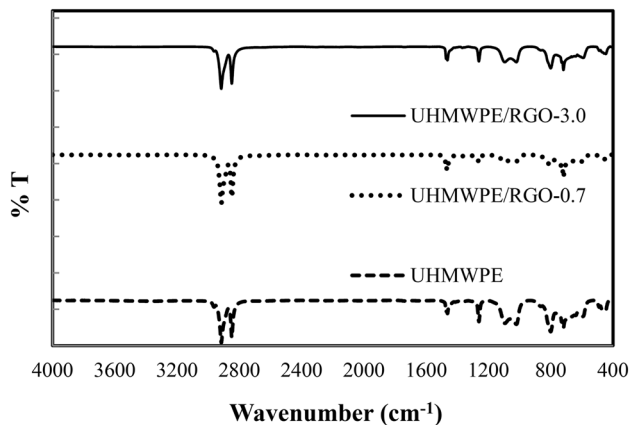


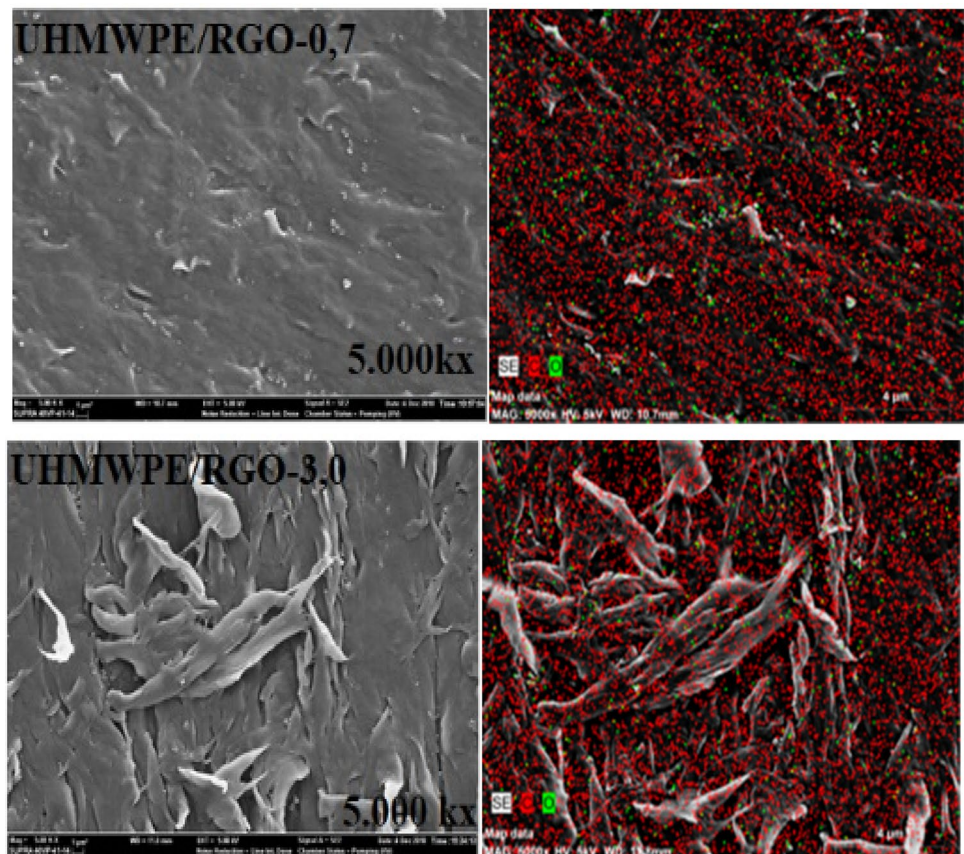
Fig. 1 XRD patterns of unfilled UHMWPE and UHMWPE/RGO biocomposites

3.0 wt% RGO filling reduced the intensity of both UHMWPE peaks, which could be attributed to modification of matrix crystallinity [20]. The values of crystallite size of unfilled UHMWPE and UHMWPE/RGO biocomposites for  $2\theta = 23.92^\circ$ , were shown in Fig. 1. It is observed that 0.7 wt% RGO contents results in increase of crystallite size achieving 100%, for comparison biocomposite with 3.0 wt% RGO and unfilled polymer. The increase of



**Fig. 2** FTIR spectrum of unfilled UHMWPE and UHMWPE/RGO biocomposites

**Fig. 3** SEM micrographs of unfilled UHMWPE and UHMWPE/RGO biocomposites; EDS elemental map of Carbon and Oxygen



crystalline size in the UHMWPE/RGO-0.7 biocomposite and subsequently will affect the wear behavior of the biocomposite. Because the low RGO amount was act as nucleation centers and not disruptive reorganization and chain folding during crystallization process [21]. Additionally, there is no new diffraction peak were observed in the patterns of biocomposites except the orthorhombic crystal peaks of unfilled polymer. This clearly indicated that RGO was exfoliated in the UHMWPE matrix [4, 22].

Figure 2 showed the FTIR spectra of the UHMWPE and UHMWPE/RGO biocomposites. The peaks of  $2915.92\text{ cm}^{-1}$ ,  $2848.69\text{ cm}^{-1}$ ,  $1463.04\text{ cm}^{-1}$  and  $718.47\text{ cm}^{-1}$  were attributed to the CH asymmetric vibration, the CH symmetric vibration, the  $\text{CH}_2$  the bending vibration and  $\text{CH}_2$  rocking vibration, respectively, for the unfilled UHMWPE. The strength of the peaks at  $2915.92\text{ cm}^{-1}$ ,  $2848.69\text{ cm}^{-1}$ ,  $1463.04\text{ cm}^{-1}$  and  $718.47\text{ cm}^{-1}$  enhanced with low and high amounts of RGO, which possibly indicated that more interaction between RGO and UHMWPE matrix [23].

Figure 3 showed the SEM images of the surfaces of UHMWPE/RGO biocomposites with different amounts of RGO and EDS elemental map of carbon and oxygen. It could be seen that the surface of UHMWPE/RGO-0.7 was relatively flat but also it had uneven regions. The image of this biocomposite showed RGO were embedded into the

UHMWPE matrix so that good interfacial bonding strength exhibited between RGO and UHMWPE [14]. Furthermore, as the content of RGO increased to 3.0 wt%, the morphology of the surface was totally different. The UHMWPE/RGO-3.0 biocomposite exhibited an obviously rough and deformed morphology. As a result, the reorganization and chain folding of the polymer was hindered by the increasing content of RGO. In the XRD analysis section discussed the low amount of the RGO that caused nucleation centers by using crystallite size data. The EDS elemental mapping of biocomposites confirms that oxygen was uniformly distributed in the biocomposites. The dispersion of oxygen is very important because only RGO have oxygen containing functional groups. The results obtained from the EDS are compatible with XRD results.

Table 1 showed that the microhardness, wear rate and friction coefficient values of unfilled UHMWPE and biocomposites under distilled water lubricating condition. Hardness of the biocomposites increased at all RGO loading content and when the loading content is 0.7 wt%, biocomposite had the best microhardness value in contrast to that of unfilled UHMWPE. The distribution of RGO in polymer matrix, as discussed in EDS analysis and XRD sections, may result in an increase of resistance to indentation [18]. It could be seen that the wear rate of all the biocomposites filled with RGO were lower than that of unfilled UHMWPE. Also, it was observed that the low amount of RGO that resulted in the maximum wear resistance. These results may be attributed to the excellent mechanical properties and high specific surface area of RGO, which facilitates good load transfer to the RGO network [12]. It could be seen that after adding the content of RGO into UHMWPE matrix, the friction coefficient of biocomposites decreased significantly. Both RGO and distilled water displayed lubricant properties because of homogeneous dispersion of RGO in the UHMWPE matrix and good interaction of filler and polymer matrix according to XRD, EDS and FTIR analysis results [15, 24].

**Table 1** Microhardness, wear rate and friction coefficient values of UHMWPE and UHMWPE/RGO biocomposites

Samples	Microhardness (MPa)	Wear rate $\times 10^{-4}$ (mm <sup>3</sup> /Nm)	Friction coefficient
UHMWPE	5.86	5.62	0.089
UHMWPE/RGO-0.7	6.41	5.24	0.058
UHMWPE/RGO-3.0	6.09	5.45	0.056

Figure 4 showed the effects of different amount of RGO on the worn surface of biocomposites. In the low magnified image, it could be seen that the worn surface of unfilled UHMWPE were thin and superficial grooves under deionized water. The fatigue wear was found dominant where the cracked surface layer of the unfilled UHMWPE in the high magnified image. The low and high magnified images of UHMWPE/RGO-0.7 showed that the wear marks due to the grooves were disappeared and lead to severe adhesive wear. When the RGO filler loading was increased to 3.0 wt% the worn surfaces seemed to be severe adhesive wear in the low magnified image. Additionally, from the high magnified image shown in Fig. 4, it is clear that adhesive wear tracks and significant fatigue tear increased on surface of biocomposite. As a result, with the decrease in friction surface temperature, plastic deformation was not observed on the surface of biocomposites in the distilled water condition [25].

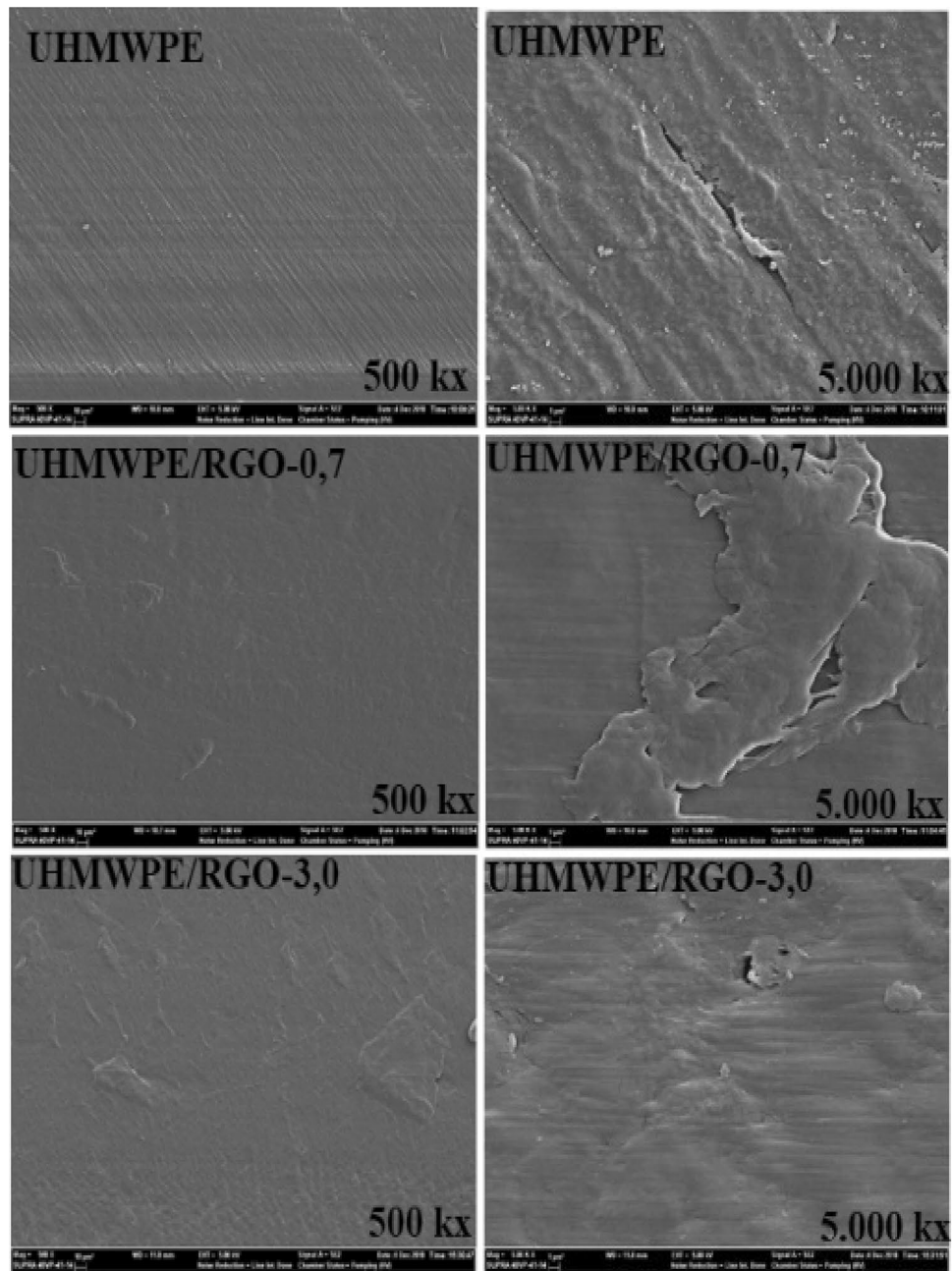
OM analyses of the morphologies of Al<sub>2</sub>O<sub>3</sub> counterface under distilled water lubricated conditions were evaluated in Fig. 5a, c. Interfacial interactions between the polymer and filler played an important role in tribofilms formation [26]. Unfilled UHMWPE have a thin and uniform transfer film on the Al<sub>2</sub>O<sub>3</sub> ball (Fig. 5a). When sliding occurred under distilled water lubricated condition, a robust tribofilm generated from UHMWPE/RGO-3.0 (Fig. 5c) and a patchy tribofilm produced from UHMWPE/RGO-0.7 were observed (Fig. 5b), which led to a lower wear rate of biocomposite with 0.7 wt% of RGO than that of biocomposite with 3.0 wt% of RGO. The strongly interfacial interactions between UHMWPE with RGO and high crystallite size amount of UHMWPE/RGO-0.7 biocomposite under distilled water condition was prone to destroy the tribofilm formed on Al<sub>2</sub>O<sub>3</sub> surface.

## 4 Conclusions

RGO filled UHMWPE biocomposites were successfully fabricated and assessed in terms of tribological performance under distilled water lubrication condition. The following conclusions can be obtained from above studies.

- FTIR results showed that there was interaction between the RGO and UHMWPE. It could be affirmed homogeneous dispersion of the RGO in the UHMWPE matrix

**Fig. 4** SEM micrographs of worn surfaces of the unfilled UHMWPE and biocomposites



and crystallite size achieving 100% in UHMWPE/RGO-0.7 biocomposite as confirmed by XRD analysis.

- SEM images showed that RGO were embedded into the UHMWPE matrix so that good interfacial bonding strength exhibited between RGO and UHMWPE in UHMWPE/RGO-0.7 biocomposite. The EDS elemental

mapping of biocomposites confirms that oxygen was uniformly distributed in the all biocomposites.

- The addition of RGO with small amounts was obviously increased the microhardness and the biocomposite with 0.7 wt% RGO had the best microhardness value.
- The fatigue wear tracks and wear rate were significantly reduced when RGO was added up to 0.7 wt%.

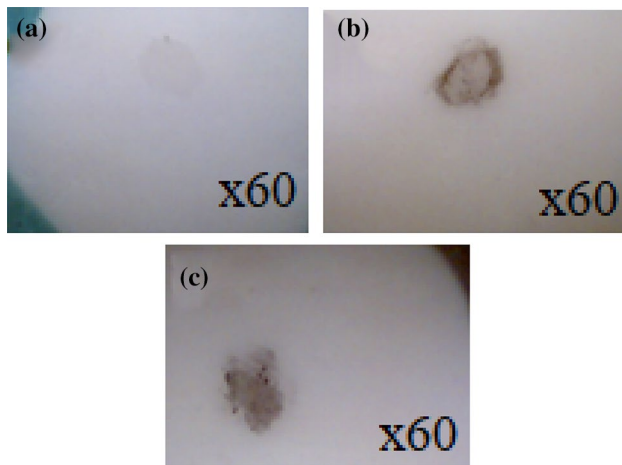


**Fig. 5** OM images of the  $\text{Al}_2\text{O}_3$  balls sliding against the **a** unfilled UHMWPE, **b** UHMWPE/RGO-0.7 and **c** UHMWPE/RGO-3.0 biocomposites

- With the RGO content increases, the frictional coefficient of the biocomposites were decreased. It is due to an efficient load transfer from the matrix to the filler.

### Compliance with ethical standards

**Conflict of interest** The authors declare that they have no conflict of interest.

### References

- Shi G, Cao Z, Yan X, Wang Q (2019) In-situ fabrication of a UHMWPE nanocomposite reinforced by  $\text{SiO}_2$  nanospheres and its tribological performance. *Mater Chem Phys* 236:1–9. <https://doi.org/10.1016/j.matchemphys.2019.121778>
- Zoo Y-S, An J-W, Lim D-P, Lim D-S (2004) Effect of carbon nanotube addition on tribological behavior of UHMWPE. *Tribol Lett* 16:305–309. <https://doi.org/10.1023/B:TRIL.0000015206.21688.87>
- Melk L, Emami N (2018) Mechanical and thermal performances of UHMWPE blended vitamin E reinforced carbon nanoparticle composites. *Compos B* 146:20–27. <https://doi.org/10.1016/j.compositesb.2018.03.034>
- Pang W, Ni Z, Chen G, Huang G, Huang H, Zhao Y (2015) Mechanical and thermal properties of graphene oxide/ultra-high molecular weight polyethylene nanocomposites. *RSC Adv* 77:63063–63072. <https://doi.org/10.1039/C5RA11826C>
- Tai Z, Chen Y, An Y, Yan X, Xue Q (2012) Tribological behavior of UHMWPE reinforced with graphene oxide nanosheets. *Tribol Lett* 46:55–63. <https://doi.org/10.1007/s11249-012-9919-6>
- Salari M, Taromsari SM, Reza Bagheri, Sani MAF (2019) Improved wear, mechanical, and biological behavior of UHMWPE-HAP-zirconia hybrid nanocomposites with a prospective application in total hip joint replacement. *J Mater Sci* 54:4259–4276. <https://doi.org/10.1007/s10853-018-3146-y>
- Guo Y, Sun X, Liu Yu, Wang W, Qiu H, Gao J (2012) One pot preparation of reduced graphene oxide (RGO) or Au (Ag) nanoparticle-RGO hybrids using chitosan as a reducing and stabilizing agent and their use in methanol electrooxidation. *Carbon* 50:2513–2523. <https://doi.org/10.1016/j.carbon.2012.01.074>
- Mindivan F (2015) The synthesis, thermal and structural characterization of polyvinylchloride/graphene oxide (PVC/GO) composites. *Mater Sci Non-Equilib Phase Transform* 3:33–36
- Vadukumpully S, Paul J, Mahanta N, Valiyaveetil S (2011) Flexible conductive graphene/poly(vinyl chloride) composite thin films with high mechanical strength and thermal stability. *Carbon* 49:198–205. <https://doi.org/10.1016/j.carbon.2010.09.004>
- Sandhya PK, Jose J, Sreekala MS, Padmanabhan M, Kalarikkal N (2018) Reduced graphene oxide and ZnO decorated graphene for biomedical applications. *Ceram Int* 44:15092–15098. <https://doi.org/10.1016/j.ceramint.2018.05.143>
- Vadivel HS, Golchin A, Emami N (2018) Tribological behaviour of carbon filled hybrid UHMWPE composites in water. *Tribol Int* 124:169–177. <https://doi.org/10.1016/j.triboint.2018.04.001>
- Pang W, Ni Z, Wu JL, Zhao Y (2018) Investigation of tribological properties of graphene oxide reinforced ultrahigh molecular weight polyethylene under artificial seawater lubricating condition. *Appl Surf Sci* 434:273–282. <https://doi.org/10.1016/j.apsusc.2017.10.115>
- Golchin A, Wikner A, Emami N (2016) An investigation into tribological behaviour of multi-walled carbon nanotube/graphene oxide reinforced UHMWPE in water lubricated contacts. *Tribol Int* 95:156–161. <https://doi.org/10.1016/j.triboint.2015.11.023>
- Chih A, Anson-Casaos A, Puertolas JA (2017) Frictional and mechanical behaviour of graphene/UHMWPE composite coatings. *Tribol Int* 116:295–302. <https://doi.org/10.1016/j.triboint.2017.07.027>
- Aliyu IK, Mohammed AS, Al-Qutub A (2018) Tribological performance of ultra high molecular weight polyethylene nanocomposites reinforced with graphene nanoplatelets. *Polym Compos* 40:1301–1311. <https://doi.org/10.1002/pc.24975>
- Bhattacharyya A, Chen S, Zhu M (2014) Graphene reinforced ultra high molecular weight polyethylene with improved tensile strength and creep resistance properties. *Express Polym Lett* 8(2):74–84. <https://doi.org/10.3144/expresspolymlett.2014.10>
- Hummers WS, Offeman RE (1958) Preparation of graphitic oxide. *J Am Chem Soc* 6(80):1339. <https://doi.org/10.1021/ja01539a017>
- Mindivan F, Gökaş M (2019) Preparation of new PVC composite using green reduced graphene oxide and its effects in thermal and mechanical properties. *Polym Bull* 2019:1–21. <https://doi.org/10.1007/s00289-019-02831-x>
- Mohammed AS, Ali A, Nesar M (2017) Evaluation of tribological properties of organoclay reinforced UHMWPE nanocomposites. *J Tribol* 139:1–6. <https://doi.org/10.1115/1.4033188>
- Ahmad M, Uzir Wahit M, Rafiq Abdul Kadir M, Zaman Mohd Dahlan K (2012) Mechanical, rheological, and bioactivity properties of ultra high-molecular-weight polyethylene bioactive composites containing polyethylene glycol and hydroxyapatite. *Sci World J* 2012:1–13. <https://doi.org/10.1100/2012/474851>
- Amangah M, Salami-Kalajahi M, Roghani-Mamaqani H (2018) Nanoconfinement effect of graphene on thermophysical properties and crystallinity of matrix-grafted graphene/crosslinked polysulfide polymer nanocomposites. *Diam Relat Mater* 83:177–183. <https://doi.org/10.1016/j.diamond.2018.02.012>
- Bahrani H, Ramazani SAA, Kheradmand A, Shafiee M, Baniasadi H (2015) Investigation of thermomechanical properties of UHMWPE/Graphene oxide nanocomposites prepared by

- in situ Ziegler-Natta polymerization. *Adv Polym Technol.* <https://doi.org/10.1002/adv.21508>
23. Kandhol G, Wadhwa H, Chand S, Mahendia S, Kumar S (2019) Study of dielectric relaxation behavior of composites of Poly(vinyl alcohol) (PVA) and reduced graphene oxide (RGO). *Vacuum* 160:384–393. <https://doi.org/10.1016/j.vacuum.2018.11.051>
  24. Huang G, Ni Z, Chen G, Zhao Y (2016) The influence of irradiation and accelerated aging on the mechanical and tribological properties of the graphene oxide/ultra-high-molecular-weight polyethylen nanocomposites. *Int J Polym Sci* 2016:1–9. <https://doi.org/10.1155/2016/2618560>
  25. Dong P, Long C, Peng Y, Peng X, Guo F (2019) Effect of coatings on thermal conductivity and tribological properties of aluminum foam/polyoxymethylene interpenetrating composites. *J Mater Sci* 54:13135–13146. <https://doi.org/10.1007/s10853-019-03826-9>
  26. Qi H, Hu C, Zhang G, Yu J, Zhang Y, He H (2019) Comparative study of tribological properties of carbon fibers and aramid particles reinforced polyimide composites under dry and sea water lubricated conditions. *Wear* 436–437:1–9. <https://doi.org/10.1016/j.wear.2019.203001>

**Publisher's Note** Springer Nature remains neutral with regard to jurisdictional claims in published maps and institutional affiliations.